Monthly Notices
of the
ROYAL ASTRONOMICAL SOCIETY

Mon. Not. R. Astron. Soc. **412,** 1381–1388 (2011) doi:10.1111/j.1365-2966.2010.17995.x

Non-linear electromagnetic waves in magnetosphere of a magnetar

Dan Mazur and Jeremy S. Heyl★†

Department of Physics and Astronomy, University of British Columbia, Vancouver, BC V6T 1Z1, Canada

Accepted 2010 November 8. Received 2010 October 25; in original form 2010 June 29

ABSTRACT

We compute electromagnetic wave propagation through the magnetosphere of a magnetar. The magnetosphere is modelled as the quantum electrodynamics vacuum and a cold, strongly magnetized plasma. The background field and electromagnetic waves are treated non-perturbatively and can be arbitrarily strong. This technique is particularly useful for examining non-linear effects in propagating waves. Waves travelling through such a medium typically form shocks; on the other hand we focus on the possible existence of waves that travel without evolving. Therefore, in order to examine the non-linear effects, we make a travelling wave ansatz and numerically explore the resulting wave equations. We discover a class of solutions in a homogeneous plasma which are stabilized against forming shocks by exciting non-orthogonal components which exhibit strong non-linear behaviour. These waves may be an important part of the energy transmission processes near pulsars and magnetars.

Key words: magnetic fields – plasmas – shock waves – waves – stars: magnetars.

1 INTRODUCTION

The magnetosphere of a magnetar provides a particularly interesting medium for the propagation of electromagnetic waves. Magnetars are characterized by exceptionally large magnetic fields that can be several times larger than the quantum critical field strength (Mereghetti 2008). Because the magnetic fields are so large, the fluctuations of the vacuum of quantum electrodynamics (QED) influence the propagation of light. Specifically, the vacuum effects add non-linear terms to the wave equations of light in the presence large magnetic fields. In addition, the magnetosphere of a magnetar contains a plasma which alters the dispersion relationship for light. Because of the unique optical conditions in the magnetospheres of magnetars, they provide excellent arenas to explore non-linear vacuum effects arising due to QED.

The influence of QED vacuum effects from strong magnetic fields in the vicinities of magnetized stars has previously been studied by several authors. The combined QED vacuum and plasma medium is discussed in detail in the context of neutron stars in Mészáros (1992). Vacuum effects have been found to dominate the polarization properties and transport of X-rays in the strong magnetic fields near neutron stars (Mészáros & Ventura 1978, 1979; Meszaros, Nagel & Ventura 1980; Meszaros & Bonazzola 1981; Galtsov & Nikitina 1983). Detailed consideration of magnetic vacuum effects is therefore critical to an understanding of emissions from highly magnetized stars.

Most studies of waves in systems including plasmas or vacuum effects approach the problem perturbatively, which limits the applicability of their results. The purpose of the present paper is to examine the combined impact of the QED vacuum and a magnetized plasma using non-perturbative methods to fully preserve the non-linear interaction between the fields. Neutron stars may be capable of producing very intense electromagnetic waves, comparable to the ambient magnetic field. For example, a coupling between plasma waves and seismic activity in the crust could produce an Alfvén wave with a very large amplitude (Blaes et al. 1989; Thompson & Duncan 1995). Even if they may not be produced directly, electromagnetic waves naturally develop through the interactions between Alfvén waves. To lowest order in the size of the wave, Alfvén waves do not suffer from shock formation (Thompson & Blaes 1998) whereas electromagnetic waves do (Heyl & Hernquist 1998, 1999); therefore, how to stabilize the propagation of the latter is the focus of this paper.

If such a magnetospheric disturbance results in electromagnetic waves of sufficiently large amplitude and low frequency, then non-perturbative techniques are required to characterize the wave. The importance of studying such a system non-perturbatively is particularly well illustrated by the fact that some non-linear wave behaviour is fundamentally non-perturbative, as is generally the case with solitons (Rajaraman 1982). In order to handle the problem non-perturbatively, we choose to study waves whose space–time dependence is described by the parameter $S = x - vt$, where v is a constant speed of propagation through the medium in the $\hat{\boldsymbol{x}}$-direction . In the study of waves, one normally chooses the ansatz $e^{i(\omega t - \boldsymbol{k}\cdot\boldsymbol{x})}$. However, in this picture, a numerical study would typically treat the self-interactions of the electromagnetic field by summing the interactions of finitely many Fourier modes. So, this ansatz

★E-mail: heyl@phas.ubc.ca
†Canada Research Chair.

conflicts with our goal of studying the non-linear interactions to all orders. In contrast, a plane wave ansatz given by $S = x - vt$ allows us to study a simple wave structure to all orders without any reference to individual Fourier modes.

We model a magnetar atmosphere by including the effects of arbitrarily strong electromagnetic fields using a QED one-loop effective Lagrangian approach. These effects are discussed in Section 2.2. Plasma effects are included by assuming free electrons moving under the Lorentz force without any self-interactions. The model is that of a cold magnetohydrodynamic plasma and is discussed in Section 2.3. We have also assumed that the medium is homogeneous in agreement with the travelling-wave ansatz. Of course the actual situation is more complicated with a thermally excited plasma (e.g. Gill & Heyl 2009) and inhomogeneities — the latter can result in a whole slew of interesting interactions between the wave modes (Heyl & Shaviv 2000, 2002; Heyl, Shaviv & Lloyd 2003; Lai & Ho 2003) that are especially crucial to our understanding of the thermal radiation from their surfaces, but these are beyond the scope of this paper.

The formation of electromagnetic shocks is expected to be an important phenomenon for electromagnetic waves in the magnetized vacuum since electromagnetic waves can evolve discontinuities under the influence of non-linear interactions (Lutzky & Toll 1959; Zheleznyakov & Fabrikant 1982; Heyl & Hernquist 1998). Such shocks can form even in the presence of a plasma (Heyl & Hernquist 1999). In this study, through our explicit focus on travelling waves, we examine an alternate class of solutions to the wave equations which do not suffer this fate. Instead, they are stabilized against the formation of discontinuities by non-linear features. These waves travel as periodic wave trains without any change to their form, such as wave steepening or shock formation. Waves such as these may contribute to the formation of pulsar microstructures (Chian & Kennel 1987; Jenet, Anderson & Prince 2001).

2 WAVE EQUATIONS

2.1 The Maxwell's equations

The vacuum of QED in the presence of large magnetic fields can be described as a non-linear optical medium (Heyl & Hernquist 1997b). We also choose to treat the effect of the plasma on the waves through source terms $\rho_{\rm p}$ and $\boldsymbol{J}_{\rm p}$; therefore, we begin by considering Maxwell's equations in the presence of a medium and plasma sources. In Heaviside–Lorentz units with $c = 1$, Maxwell's equations can be used to derive the wave equations:

$$\nabla^2 \boldsymbol{D} - \frac{\partial^2 \boldsymbol{D}}{\partial t^2} = -\nabla \times (\nabla \times (\boldsymbol{D} - \boldsymbol{E})) + \frac{\partial}{\partial t}(\nabla \times (\boldsymbol{B} - \boldsymbol{H})) + \nabla \rho_{\rm p} + \frac{\partial \boldsymbol{J}_{\rm p}}{\partial t}, \quad (1)$$

$$\nabla^2 \boldsymbol{H} - \frac{\partial^2 \boldsymbol{B}}{\partial t^2} = -\nabla(\nabla \cdot (\boldsymbol{B} - \boldsymbol{H})) - \frac{\partial}{\partial t}(\nabla \times (\boldsymbol{D} - \boldsymbol{E})) - \nabla \times \boldsymbol{J}_{\rm p}. \quad (2)$$

For clarity, we will avoid making cancellations or dropping vanishing terms. We define the vacuum dielectric and inverse magnetic permeability tensors as follows (Jackson 1975):

$$D_i = \varepsilon_{ij} E_j, \; H_i = \mu^{-1}_{ij} B_j. \quad (3)$$

In the next few sections we build a model describing travelling waves in a magnetar's atmosphere from these equations.

2.2 Vacuum dielectric and inverse magnetic permeability tensors

In this section, we describe our model of the QED vacuum in strong background fields in terms of vacuum dielectric and inverse magnetic permeability tensors. These are most conveniently described in terms of two Lorentz invariant combinations of the fields:

$$K = \left(\frac{1}{2}\varepsilon^{\lambda\rho\mu\nu} F_{\lambda\rho} F_{\mu\nu}\right)^2 = -(4\boldsymbol{E}\cdot\boldsymbol{B})^2, \quad (4)$$

$$I = F_{\mu\nu} F^{\mu\nu} = 2(|\boldsymbol{B}|^2 - |\boldsymbol{E}|^2). \quad (5)$$

In order to examine the non-linear effects of the vacuum non-perturbatively, we wish to use vacuum dielectric and inverse magnetic permeability tensors which are valid to all orders in the fields. Analytic expressions for these tensors were derived by Heyl & Hernquist (1997b) for the case of wrenchless fields ($K = -(4\,\boldsymbol{E}\cdot\boldsymbol{B})^2 = 0$) from the Heisenberg–Euler–Weisskopf–Schwinger (Heisenberg & Euler 1936; Weisskopf 1936; Schwinger 1951) one-loop effective Lagrangian in Heyl & Hernquist (1997a) and expressed in terms of a set of analytic functions:

$$X_0(x) = 4\int_0^{x/2-1} \ln(\Gamma(v+1))\,{\rm d}v + \frac{1}{3}\ln\left(\frac{1}{x}\right) + 2\ln 4\pi - 4\ln A - \frac{5}{3}\ln 2 - \left[\ln 4\pi + 1 + \ln\left(\frac{1}{x}\right)\right]x + \left[\frac{3}{4} + \frac{1}{2}\ln\left(\frac{2}{x}\right)\right]x^2, \quad (6)$$

$$X_1(x) = -2X_0(x) + xX_0^{(1)}(x) + \frac{2}{3}X_0^{(2)}(x) - \frac{2}{9}\frac{1}{x^2}, \quad (7)$$

$$X_2(x) = -24X_0(x) + 9xX_0^{(1)}(x) + (8+3x^2)X_0^{(2)}(x) + 4xX_0^{(3)}(x) - \frac{8}{15}X_0^{(4)}(x) + \frac{8}{15}\frac{1}{x^2} + \frac{16}{15}\frac{1}{x^4}, \quad (8)$$

where

$$X_0^{(n)}(x) = \frac{{\rm d}^n X_0(x)}{{\rm d}x^n} \quad (9)$$

and

$$\ln A = \frac{1}{12} - \zeta^{(1)}(-1) = 0.248754477. \quad (10)$$

The tensors we need are derived in Heyl & Hernquist (1997b), except that we have kept terms up to linear order in the expansion about $K = 0$ instead of dealing with the strictly wrenchless case. Our analysis therefore requires that $K \ll B_k^4$:

$$\varepsilon^{ij} = \Delta^{ij} - \frac{\alpha}{2\pi}\left[\frac{2}{I}X_1\left(\frac{1}{\xi}\right) + \frac{12K}{I^3}X_2\left(\frac{1}{\xi}\right)\right]B^i B^j, \quad (11)$$

$$(\mu^{-1})^{ij} = \Delta^{ij} + \frac{\alpha}{2\pi}\left[\frac{2}{I}X_1\left(\frac{1}{\xi}\right) + \frac{K}{12I^3}X_2\left(\frac{1}{\xi}\right)\right]E^i E^j, \quad (12)$$

where

$$\Delta^{ij} = \delta^{ij}\left[1 + \frac{\alpha}{2\pi}\left(-2X_0\left(\frac{1}{\xi}\right) + \frac{1}{\xi}X_0^{(1)}\left(\frac{1}{\xi}\right) + \frac{K}{4I^2}X_1\left(\frac{1}{\xi}\right) + \frac{K}{8I^2\xi}X_1^{(1)}\left(\frac{1}{\xi}\right)\right)\right], \quad (13)$$

the fine-structure constant is $\alpha = e^2/4\,\pi$ in these units where we have set $\hbar = c = 1$, and

$$\xi = \frac{1}{B_k}\sqrt{\frac{I}{2}}. \tag{14}$$

Equations (11) and (12) define our model for the QED vacuum in a strong electromagnetic field. Because we will focus on photon energies much lower than the rest-mass energy of the electron, we have treated the vacuum as strictly non-linear. It is not dispersive. The treatment of the dispersive properties of the vacuum would require an effective action treatment (e.g. Cangemi, D'hoker & Dunne 1995a,b) rather than the local effective Lagrangian treatment used here.

2.3 Plasma

To investigate travelling waves, we choose our coordinate system so that the $\hat{\boldsymbol{x}}$-direction is aligned with the direction of propagation. Then, the space–time dependence of the fields and sources is given by a single parameter $S \equiv x - vt$, where v is the constant phase velocity in the $\hat{\boldsymbol{x}}$-direction of the travelling wave. At this point, we are choosing to work in a specific Lorentz frame.

We model the plasma as a free electron plasma which enters the wave equation through the source terms ρ_p and $\boldsymbol{J}_\mathrm{p}$. For electromagnetic fields obeying the travelling wave ansatz, the sources must also obey the ansatz. Then, ρ_p and $\boldsymbol{J}_\mathrm{p}$ are functions only of S. We therefore treat them as an additional field which is integrated along with the electromagnetic components of the field.

In order to perform the numerical ordinary differential equation (ODE) integration for the currents, we wish to find expressions for $\mathrm{d}\rho_\mathrm{p}/\mathrm{d}S$ and $\mathrm{d}\boldsymbol{J}_\mathrm{p}/\mathrm{d}\,S$. For travelling waves, the continuity equation is

$$-v\frac{\mathrm{d}\rho_\mathrm{p}}{\mathrm{d}S} + \delta^{ix}\frac{\mathrm{d}J^i_\mathrm{p}}{\mathrm{d}S} = 0, \tag{15}$$

where we are using index notation to label our explicitly Cartesian $\{x, y, z\}$ coordinate system. Repeated indices are summed. However, whenever x or z appears as an index, it is fixed and does not run from 1 to 3.

We use equation (15) to rewrite the source terms from equation (1):

$$\partial^i\rho_\mathrm{p} + \frac{\partial J^i_\mathrm{p}}{\partial t} = \frac{1}{v}\frac{\mathrm{d}J^i_\mathrm{p}}{\mathrm{d}S}(\delta^{ix} - v^2). \tag{16}$$

Similarly, the source term from equation (2) is

$$(\nabla \times J_\mathrm{p})^i = \varepsilon^{ixk}\left(\frac{\mathrm{d}J_\mathrm{p}}{\mathrm{d}S}\right)^k. \tag{17}$$

To find an expression for $\mathrm{d}\boldsymbol{J}_\mathrm{p}/\mathrm{d}S$ we express the current as an integral over the phase-space distribution of the electrons and linearize the plasma density:

$$\boldsymbol{J}_\mathrm{p} = \int f(\boldsymbol{p}_\mathrm{p})\, e\boldsymbol{v}_\mathrm{p}\mathrm{d}^3\boldsymbol{p}_\mathrm{p} \approx \bar{\gamma} ne\bar{\boldsymbol{v}}_\mathrm{p}, \tag{18}$$

where $\bar{\boldsymbol{v}}_\mathrm{p} \equiv [\int f(\boldsymbol{p}_\mathrm{p})\boldsymbol{v}_\mathrm{p}\mathrm{d}^3\boldsymbol{p}_\mathrm{p}]/\bar{\gamma}n$ and n is the mean electron density in the plasma in the reference frame where $\bar{\boldsymbol{v}}_\mathrm{p} = 0$. It is important to note the distinction between the mean plasma speed, $\bar{v}_\mathrm{p}$, and the propagation speed of the wave, v. The Lorentz factor $\bar{\gamma} \equiv 1/\sqrt{1 - \bar{v}_\mathrm{p}^2}$ accounts for a relativistic increase in the plasma density since $\mathrm{d}^3\,\boldsymbol{x} = \gamma^{-1}\,\mathrm{d}^3\,\boldsymbol{x}'$.

Next, we take a time derivative of the current and express this in terms of a three-force acting on the plasma:

$$\begin{aligned}\frac{\partial \boldsymbol{J}_\mathrm{p}}{\partial t} &= ne\frac{\partial \bar{\gamma}\bar{\boldsymbol{v}}_\mathrm{p}}{\partial t}\\ &= \frac{ne}{m}\boldsymbol{F}.\end{aligned} \tag{19}$$

Noting that $\boldsymbol{J}_\mathrm{p}$ is a function only of S, we insert the Lorentz force $\boldsymbol{F} = e(\boldsymbol{E} + \bar{\boldsymbol{v}}_\mathrm{p} \times \boldsymbol{B})$ and arrive at an expression that can be substituted into the source terms, equations (16) and (17), to find $\boldsymbol{J}_\mathrm{p}(S)$:

$$\frac{\mathrm{d}\boldsymbol{J}_\mathrm{p}}{\mathrm{d}S} = -\frac{1}{v}\frac{e}{m}(en\boldsymbol{E} + \bar{\gamma}^{-1}\boldsymbol{J}_\mathrm{p} \times \boldsymbol{B}). \tag{20}$$

The equations we have given above describe a cold, relativistic, magnetohydrodynamic plasma. Forces on the plasma arising due to pressure gradients and gravity are neglected. Moreover, in our simulations, we neglect the forces on the plasma due to the magnetic field. This approximation is suitable if the plasma in question is a pair plasma, or for wave frequencies much less than the cyclotron frequency.

As we will show in Section 4 (see Fig. 6), the field configurations generated in our simulation vary over time-scales similar to the inverse of the plasma frequency; the latter is about nine orders of magnitude smaller than the cyclotron frequency. This observation allows us to justify some aggressive assumptions regarding the plasma response. As mentioned above, we may neglect forces on the plasma from the magnetic field, and quantum effects are expected to be small far away from the cyclotron resonance (Mészáros 1992).

We also neglect thermal effects since the influence of the electromagnetic fields will dominate over thermal motion. For strong background magnetic fields such that $(eB/m) \gg kT$, the electrons will be confined to the lowest Landau level, restricting thermal motion perpendicular to the background magnetic field. As we will elaborate on in Section 4, the greatest non-linear effects occur for waves with an electric field component oriented along the background magnetic field. Because we are interested in waves with amplitudes comparable to B_k, thermal motion is negligible relative to the dynamics induced by the wave. We are therefore justified in neglecting thermal effects in every direction for the cases of greatest interest.

If one combines equation (19) with equation (1), one sees that any non-linearity in this treatment must originate with the dielectric and permeability tensors — any non-linearity that may originate from the plasma itself has been neglected (cf. Kozlov, Litvak & Suvorov 1979; Cattaert, Kourakis & Shukla 2005). The plasma is modelled as strictly dispersive. In Section 2.5, we confirm that this method of describing the plasma is consistent with standard accounts in the weak-field, small-wave limit.

2.4 Travelling wave ODEs

The wave equations for travelling waves are found by combining Maxwell's equations (1) and (2) with the continuity equation (15). We also make the plane-wave approximation, and assume that the fields and sources are described by the parameter

$$S = x - vt. \tag{21}$$

The equations governing travelling wave propagation are

$$\frac{\mathrm{d}^2\psi^i(S)}{\mathrm{d}S^2} = \frac{1}{v}\frac{\mathrm{d}J^i(S)}{\mathrm{d}S}(\delta^{ix} - v^2), \tag{22}$$

$$\frac{\mathrm{d}^2\chi^i(S)}{\mathrm{d}S^2} = -\varepsilon^{ixj}\frac{\mathrm{d}J^j(S)}{\mathrm{d}S}. \tag{23}$$

The auxiliary vectors ψ^i and χ^i are related to the electric and magnetic fields:

$$\begin{aligned}\psi^i(S) = {} & (1-v^2)\varepsilon^{ij}E^j + \delta^{ix}(\varepsilon^{xj}E^j - E^x) \\ & -(\varepsilon^{ij}E^j - E^i) + \varepsilon^{ixk}v(B^k - (\mu^{-1})^{kj}B^j),\end{aligned} \tag{24}$$

$$\begin{aligned}\chi^i(S) = {} & ((\mu^{-1})^{ij}B^j - v^2B^i) + \delta^{ix}(B^x - (\mu^{-1})^{xj}B^j) \\ & -\varepsilon^{ixk}v(\varepsilon^{kj}E^j - E^k).\end{aligned} \tag{25}$$

Equations (22) through (25) define a set of coupled ODEs that can be integrated to solve for the travelling electric and magnetic fields. Solving these equations requires that we have at hand the vacuum dielectric and inverse magnetic permeability tensors as well as an expression for $\mathrm{d}\,\boldsymbol{J}_\mathrm{p}/\mathrm{d}S$. These were discussed in Sections 2.2 and 2.3, respectively.

2.5 Weak field, small wave limit

In this section, we would like to demonstrate that our equations reduce to standard expressions in the case of small background fields and small electromagnetic waves. To make this comparison, it is also prudent to assume waves have a space–time dependence like $\mathrm{e}^{\mathrm{i}(\omega t - \boldsymbol{k}\cdot\boldsymbol{x})}$ instead of $x - vt$. By making this change, we can compare our other assumptions with those made in standard textbook accounts directly.

Under the assumption that the fields and currents have the standard plane-wave space–time dependence, we can make the replacements $(\partial/\partial t) \rightarrow -\mathrm{i}\omega$ and $\nabla \rightarrow \mathrm{i}\boldsymbol{k}$. We can then write a second expression for $\partial\boldsymbol{J}/\partial\, t$:

$$\frac{\partial \boldsymbol{J}_\mathrm{p}}{\partial t} = -\mathrm{i}\omega\boldsymbol{J}_\mathrm{p}. \tag{26}$$

Setting equations (26) and (19) equal, we get

$$\frac{e}{m}(\varepsilon^{ijk}J_\mathrm{p}^j B^k) + \mathrm{i}\omega J_\mathrm{p}^i = \frac{e^2}{m}nE^i, \tag{27}$$

where we have used the non-relativistic approximation, which is appropriate for small waves. We will now specialize to a background magnetic field pointing in the $\hat{z}$-direction. We can then write this background field in terms of the cyclotron frequency $\omega_\mathrm{c} = eB/m$. The density n determines the plasma frequency $\omega_\mathrm{p}^2 = n\,(e^2/m)$. Then, we can write equation (27) as

$$\left[-\omega_\mathrm{c}\varepsilon^{ijz} - \mathrm{i}\omega\delta^{ji}\right] J_\mathrm{p}^j = \omega_\mathrm{p}^2 E^i. \tag{28}$$

We can solve this for $\boldsymbol{J}_\mathrm{p}$ by writing a matrix equation:

$$\boldsymbol{J}_\mathrm{p} = \begin{pmatrix} -\mathrm{i}\omega & -\omega_\mathrm{c} & 0 \\ \omega_\mathrm{c} & -\mathrm{i}\omega & 0 \\ 0 & 0 & -\mathrm{i}\omega \end{pmatrix}^{-1} \omega_\mathrm{p}^2\boldsymbol{E}, \tag{29}$$

inverting the matrix gives

$$\boldsymbol{J}_\mathrm{p} = \begin{pmatrix} \dfrac{\mathrm{i}\omega}{\omega^2-\omega_\mathrm{c}^2} & \dfrac{-\omega_\mathrm{c}}{\omega^2-\omega_\mathrm{c}^2} & 0 \\ \dfrac{\omega_\mathrm{c}}{\omega^2-\omega_\mathrm{c}^2} & \dfrac{\mathrm{i}\omega}{\omega^2-\omega_\mathrm{c}^2} & 0 \\ 0 & 0 & \mathrm{i}/\omega \end{pmatrix} \omega_\mathrm{p}^2\boldsymbol{E}. \tag{30}$$

Finally, we would like to use equation (30) to write the right-hand side of equation (1) in the small wave limit in a manner we can interpret as a dielectric tensor.

Ignoring (for now) the contributions from the vacuum, and assuming an approximately homogeneous plasma density, equation (1) simplifies to

$$\begin{aligned}\nabla^2\boldsymbol{E} - \frac{\partial^2\boldsymbol{E}}{\partial t^2} &= \frac{\partial \boldsymbol{J}_\mathrm{p}}{\partial t} \\ &= -\mathrm{i}\omega\boldsymbol{J}_\mathrm{p}.\end{aligned} \tag{31}$$

If our macroscopic field is to obey $\nabla^2\boldsymbol{D} - (\partial^2\boldsymbol{D}/\partial t^2) = 0$, we can insert equation (30) into equation (31) to obtain the following expression for the dielectric tensor due to plasma effects:

$$\varepsilon_{ij}^{(\mathrm{p})} = \begin{pmatrix} 1 - \dfrac{\omega_\mathrm{p}^2}{\omega^2-\omega_\mathrm{c}^2} & -\mathrm{i}\dfrac{\omega_\mathrm{c}}{\omega}\dfrac{\omega_\mathrm{p}^2}{\omega^2-\omega_\mathrm{c}^2} & 0 \\ \mathrm{i}\dfrac{\omega_\mathrm{c}}{\omega}\dfrac{\omega_\mathrm{p}^2}{\omega^2-\omega_\mathrm{c}^2} & 1 - \dfrac{\omega_\mathrm{p}^2}{\omega^2-\omega_\mathrm{c}^2} & 0 \\ 0 & 0 & 1 - \left(\dfrac{\omega_\mathrm{p}^2}{\omega^2}\right) \end{pmatrix}. \tag{32}$$

This expression is in agreement with the cold plasma dielectric tensor given in Mészáros (1992). As noted above, our analysis neglects the off-diagonal (Hall) terms, as is appropriate for pair plasmas or waves with frequencies much less than the cyclotron frequency.

Because the vacuum effects are added explicitly in the form of dielectric and magnetic permeability tensors, we only need to confirm that the weak field limits of our expressions agree with the standard results. This confirmation is done explicitly in Heyl & Hernquist (1997b).

In the weak field limit, the tensors given by equations (11) and (12) are

$$\varepsilon_{ij}^{(\mathrm{v})} = \delta_{ij} + \frac{1}{45\pi}\frac{\alpha}{B_k^2}\left[2(E^2 - B^2)\delta_{ij} + 7B_iB_j\right], \tag{33}$$

$$\mu_{ij}^{-1(\mathrm{v})} = \delta_{ij} + \frac{1}{45\pi}\frac{\alpha}{B_k^2}\left[2(E^2 - B^2)\delta_{ij} - 7E_iE_j\right]. \tag{34}$$

In the case of a weak background magnetic field pointing in the $\hat{z}$-direction, these become

$$\varepsilon_{ij}^{(\mathrm{v})} = \begin{pmatrix} 1-2\delta & 0 & 0 \\ 0 & 1-2\delta & 0 \\ 0 & 0 & 1+5\delta \end{pmatrix}, \tag{35}$$

$$\mu_{ij}^{-1(\mathrm{v})} = \begin{pmatrix} 1-2\delta & 0 & 0 \\ 0 & 1-2\delta & 0 \\ 0 & 0 & 1-6\delta \end{pmatrix} \tag{36}$$

with

$$\delta = \frac{\alpha}{45\pi}\left(\frac{B}{B_k}\right)^2. \tag{37}$$

Again, this result agrees with the vacuum tensors given in Mészáros (1992).

In this limit, we may simply add together the contributions to the dielectric tensor from the plasma and the vacuum according to

$$\varepsilon_{ij} = \delta_{ij} + (\varepsilon_{ij}^{(\mathrm{p})} - \delta_{ij}) + (\varepsilon_{ij}^{(\mathrm{v})} - \delta_{ij}) \tag{38}$$

with μ_{ij}^{-1} given entirely by the vacuum contribution.

We have thus recovered the standard result for a medium consisting of a plasma and the QED vacuum in the weak field, small wave limit.

3 SOLUTION PROCEDURE

In total, there are 15 coupled non-linear ODEs which must be integrated to produce a solution. Equations (22) and (23) define the electric and magnetic fields as functions of S. In addition, we must simultaneously integrate equation (20) which gives the plasma current as a function of S. Each of these equations has three spatial components. Initial conditions are given for each of the six field components, and the six derivatives of the field with respect to S. The equations describing the electromagnetic fields do not depend on the initial values of the current, but in principle these are the three remaining initial conditions. The ODEs are solved using a variable step-size Runge–Kutta method. In order to translate between the $\boldsymbol{E}$-and-$\boldsymbol{B}$ picture and the $\boldsymbol{\psi}$-and-$\boldsymbol{\chi}$ picture, equations (24) and (25) must be solved numerically at each time-step, including the first step when the initial conditions are given.

Tables of numerical values of the functions defined by equations (6)–(8), as well as their derivatives, were computed in advance and these were used to interpolate the values needed in the simulation using a standard cubic spline interpolation algorithm. In producing these tables, expressions for the weak and strong field limits were used in the appropriate regimes as this reduced the numerical errors.

Aside from the initial conditions for the fields and derivatives, there is one parameter in the model which must be selected. The density of the plasma, given by n in equation(18), is chosen to be

$$n = 10^{13}\,\mathrm{cm}^{-3}. \tag{39}$$

This value corresponds to the Goldreich–Julian density for a star of period $P \sim 1$ s, $\dot{P} \sim 10^{-10}$. The uniform background field is taken to equal the quantum critical field strength

$$B_k = \frac{m^2}{e} = 4.413 \times 10^{13}\,\mathrm{G}. \tag{40}$$

4 RESULTS

This study focuses on the case of waves propagating transverse to a large background magnetic field. We have already chosen the direction of propagation to be the $\hat{\boldsymbol{x}}$-direction through our definition of S in equation (21). We now choose the background magnetic field to point in the $\hat{\boldsymbol{z}}$-direction. In this situation, the largest non-linear effects occur when there is a large amplitude wave in the $\hat{\boldsymbol{z}}$ component of the electric field. This is quite natural. The values of both the dielectric tensor of the plasma (equation 32) and the weak-field limit of the vacuum dielectric tensor (equation 35) differ most from unity for this component; for strong fields the index of refraction (as well as its derivative with respect to the field strength) is largest for vacuum propagation in this mode (Heyl & Hernquist 1997b). Furthermore, the dominant three-photon interaction couples photons with the electric field pointed along the global magnetic field direction with photons whose magnetic field points along this direction. The three-point interaction for photons whose electric field is perpendicular to the magnetic field with parallel photons vanishes by the charge-parity (CP) invariance of QED (Adler 1971). Therefore, we focus on initial ($S = 0$) conditions in which the dominant component of the electric field points along the $\hat{\boldsymbol{z}}$-direction and that of the magnetic field along the $\hat{\boldsymbol{y}}$-direction.

In the classical vacuum, these initial conditions correspond to transverse, linearly polarized sine-wave solutions that travel at the speed of light. However, when the wave amplitudes are large, and there is a strongly magnetized plasma, we find that there is a deviation from normal transverse electromagnetic waves. In particular, in order to remain stable, a wave with large E_z and B_y field components must also excite waves in the E_y and B_z fields. These stabilizing wave components exhibit strong non-linear characteristics (see Figs 1 and 2). The symmetries of the wave equation require a close correspondence between the E_y and B_z waveforms as well as between the B_z and B_y waveforms. For simplicity, only one of each is plotted in the figures. The field strengths are given in units of the quantum critical field strength, B_k.

As is apparent from Fig. 1 the dominant electric field along the direction of the external magnetic field is essentially sinusoidal.

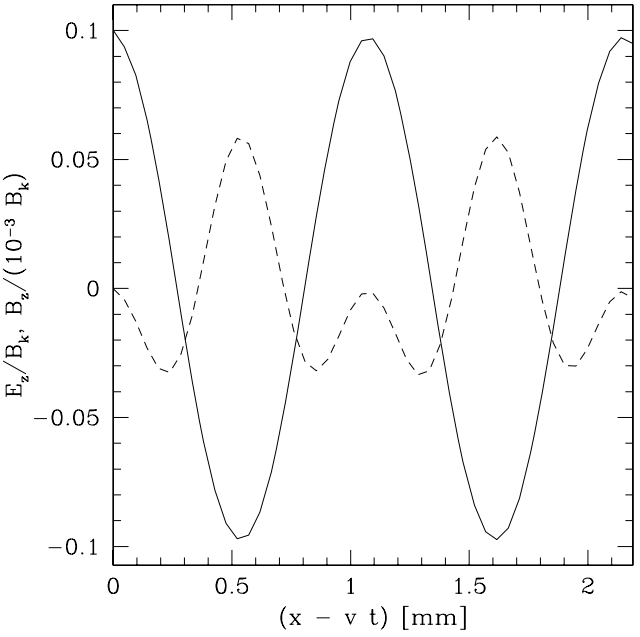

Figure 1. A comparison between the $\hat{\boldsymbol{z}}$ components of the electric (solid) and magnetic fields (dashed) showing the non-orthogonal stabilizing wave. On larger scales, the B_z component is seen to have a periodic envelope structure as in Fig. 2.

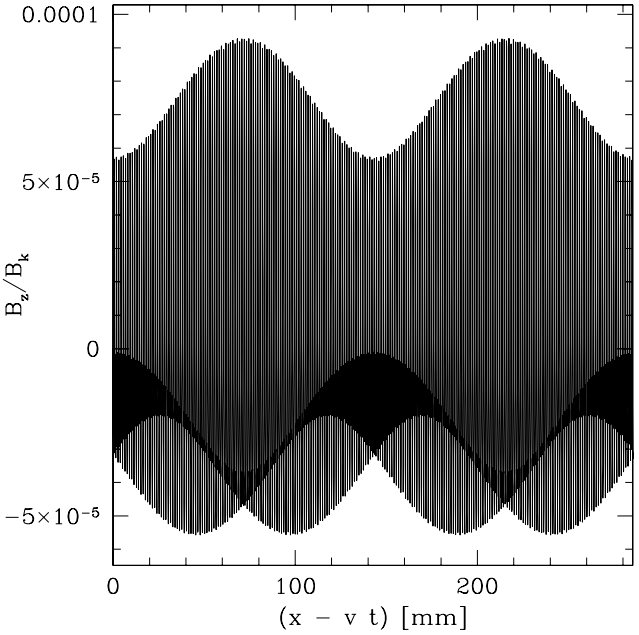

Figure 2. The B_z wave component as shown in Fig. 1 has an envelope structure when viewed at larger scales. In this case, the E_z wave component has a nearly constant amplitude of $0.1B_k$.

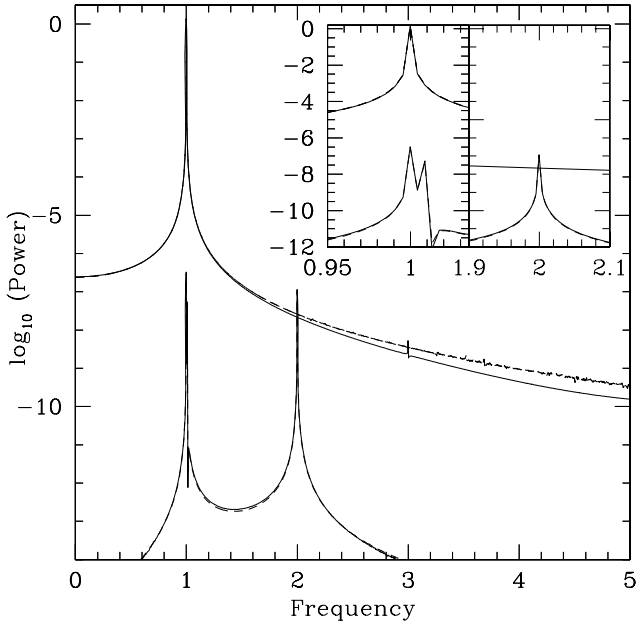

Figure 3. The solid curve depicts power spectra of the electric (upper) and magnetic fields (lower) along the $\hat{z}$-direction for the solution depicted in Figs 1 and 2. The inset focuses on the fundamental and the first harmonic. The dashed curve follows the power spectrum of a single sinusoid for the electric field and three sinusoids for the magnetic field. Near the peaks the dashed curve is essentially indistinguishable from the solid one.

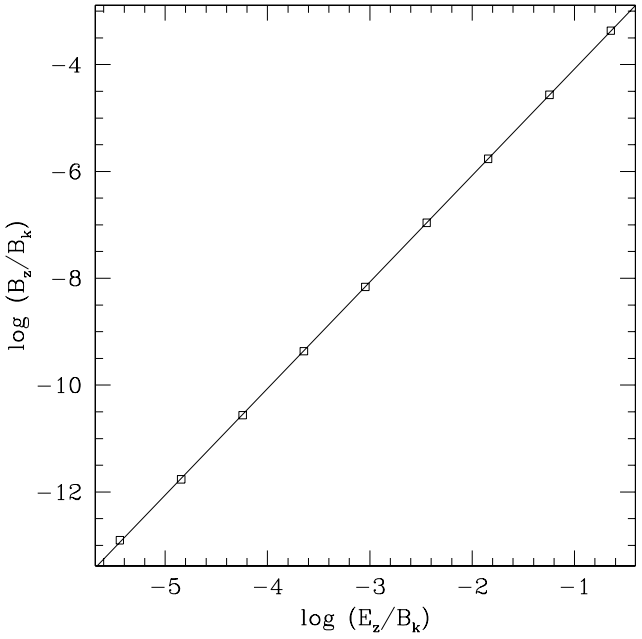

Figure 4. Amplitude of the B_z component plotted against the amplitude of the E_z component for a $B_0 = B_k$ background field. The line is the best-fitting power-law relation. The slope is consistent with a scaling exponent equal to two.

Subsequent figures will show that there is a small harmonic component. The waveform for the dominant magnetic field component is similar. On the other hand, the magnetic field along the direction of the electric field (the non-orthogonal component) is smaller by nearly four orders of magnitude and obviously exhibits higher harmonics. In particular if one expands the scale of interest (Fig. 2), the magnetic field exhibits beating between two nearby frequencies with similar power.

In order to examine the harmonic content of the waveforms, we perform fast Fourier transforms on the signals produced in the simulations. We present the results in terms of power spectra normalized by the square amplitudes of the electric field of the waves. In these plots, the horizontal axis is normalized by the frequency with the greatest power in the electric field, so that harmonics can be easily identified.

Fig. 3 depicts the power spectra of the electric and magnetic fields along the $\hat{z}$-direction for the wave depicted in Figs 1 and 2. The conclusions gathered from an examination of the waveforms are born out by the power spectra. In particular the electric field is a pure sinusoidal variation to about one part in 10 000 – the power spectrum of a pure sinusoid is given by the dashed curved. The duration of the simulation is not an integral multiple of the period of the sinusoid, resulting in a broad power spectrum even for a pure sinusoid. The power spectrum of the magnetic field follows the expectations gleaned from the waveforms. In particular the fundamental and the first harmonic are dominant, with the first harmonic having about one-third the power of the fundamental. If one focuses on the fundamental, one sees that two frequencies are involved. The envelope structure is produced by a beating between the fundamental and a slightly lower frequency with a similar amount of power as the first harmonic. Over the course of the simulation the envelope exhibits two apparent oscillations; the lower frequency differs by two frequency bins, so it is resolved separately from the fundamental as shown in the inset.

As the amplitude of the electric field increases the non-linear and non-orthogonal features of the travelling wave increase. Fig. 4 shows that the strength of the non-orthogonal magnetic field increases as the square of the electric field, a hallmark of the non-linear interaction between the fields. For the strongest waves studied with $E_z \approx 0.2B_k$ (the rightmost point in the figure), the magnetic field, B_z, is about $10^{-4}B_k$ nearly 1 per cent of the electric field. The amplitude of the non-orthogonal magnetic field is given by

$$B_z = 0.008 B_k \left(\frac{E_z}{B_k}\right)^2 \tag{41}$$

for $B_0 = B_k$. The coefficient is coincidentally very close to three-quarters of the value of the fine-structure constant. It increases with the strength of the background field.

For the strongest waves even the non-orthogonal magnetic field is strong, so it can generate non-linearities in the electric field. Although the strongest effect is around the fundamental, it is completely swamped by the fundamental of the electric field. On the other hand, the magnetic field drives a first and second harmonic in the electric field as seen in Fig. 5. The strength of these harmonics is approximately given by the formula in equation (41) or equivalently Fig. 4 if one substitutes the value of B_z for E_z and uses result for E_z. This is essentially a six-order correction from the effective Lagrangian. Because we have used the complete Lagrangian rather than a term-by-term expansion, all of the corrections up to sixth order (and further) are automatically included in the calculation.

Fig. 6 demonstrates how the frequency of the solutions varies with the speed of propagation. Because there is no mode information stored directly in our numerical solutions, we take the frequency to be rate that local minima in the electric field pass a fixed observer. In general, we find that the frequency of travelling waves increases as the phase velocity approaches the speed of light, very closely

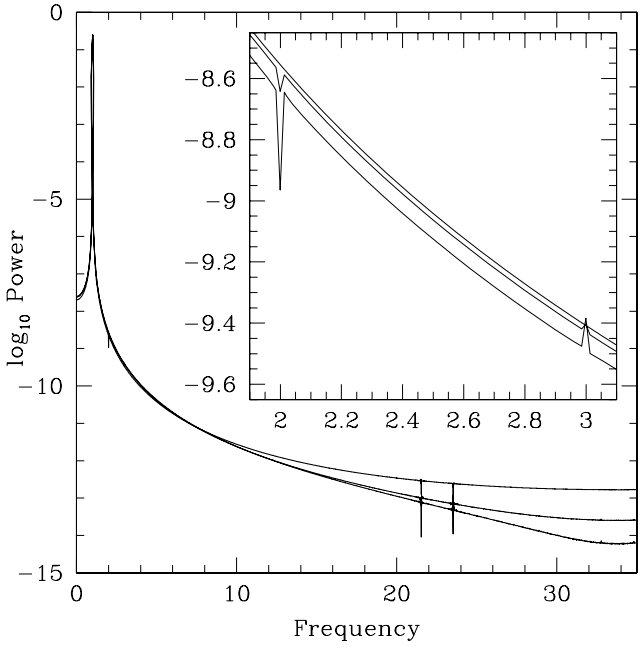

Figure 5. This power spectrum demonstrates the development of non-linear effects in the $\hat{z}$-component of the electric field as the amplitude of the wave is increased in a $B_0 = B_k$ background field. From top to bottom the curves follow the solutions whose amplitude of E_z equals 0.01, 0.08 and $0.16B_k$. The inset focuses on the first and second harmonics.

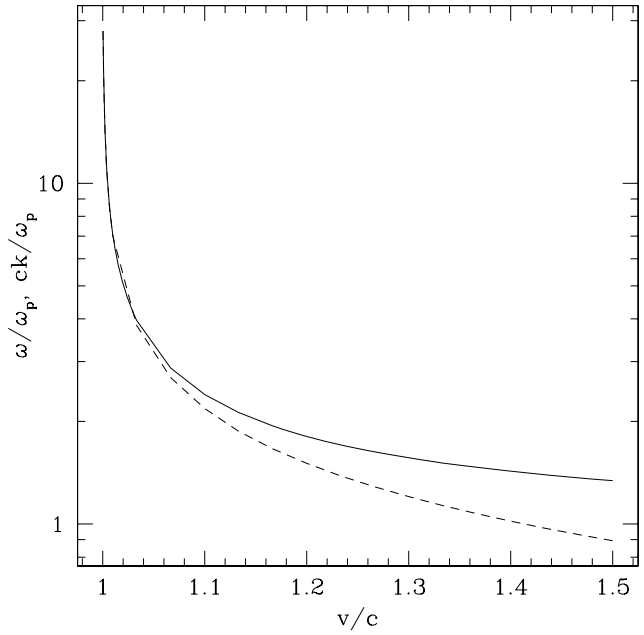

Figure 6. The frequency (solid curve) and wavenumber (dashed curve) of the travelling wave as a function of its phase velocity.

following the formula

$$\left(\frac{\omega}{\omega_{\rm p}}\right)^2 = \frac{v^2}{v^2 - 1}. \tag{42}$$

This formula also results from an analysis of the dielectric tensor, equation (32). The vacuum makes a small contribution to the wave velocity in this regime.

5 CONCLUSION

We have discussed techniques for computing electromagnetic waves in a strongly magnetized plasma which non-perturbatively account for the field interactions arising from QED vacuum effects. We applied these methods to the case of travelling waves, which have a space–time dependence given by the parameter $S = x - vt$. Travelling waves can be described without any decomposition into Fourier modes and this is ideal for exploring the non-perturbative aspects of waves.

The main result from this analysis is the observation that electromagnetic waves in a strongly magnetized plasma can self-stabilize by exciting additional non-orthogonal wave components. In the cases studied above, a large amplitude excitation of the electromagnetic field, for example, from the coupling between Alfvén waves to starquakes, can induce non-linear waves which are stabilized against the formation of shocks. The result is a periodic wave train with distinctly non-linear characteristics. Such structures may play a role in forming pulsar microstructures.

This result demonstrates that shock formation is not a necessary outcome for waves in a critically magnetized plasma. It is possible that non-linear features of a wave can stabilize it against shock formation. The shock-wave solutions generally decrease in magnitude, dissipating energy along the way unless they travel into a low-field region, so the self-stabilizing non-linear waves are the only ones that keep their shape and energy content intact as they propagate. It is not yet clear what set of conditions will determine if a particular wave will self-stabilize or collapse to form a shock or how plasma inhomogeneities will affect the propagation of a travelling wave train. These are issues that can be clarified in future work.

ACKNOWLEDGMENTS

This research was supported by funding from NSERC. The calculations were performed on computing infrastructure purchased with funds from the Canadian Foundation for Innovation and the British Columbia Knowledge Development Fund. This research has made use of NASA's Astrophysics Data System Bibliographic Services and the preprint arXiv.

REFERENCES

Adler S. L., 1971, Ann. Phys., 67, 599
Blaes O., Blandford R., Goldreich P., Madau P., 1989, ApJ, 343, 839
Cangemi D., D'hoker E., Dunne G., 1995a, Phys. Rev. D, 51, 2513
Cangemi D., D'hoker E., Dunne G., 1995b, Phys. Rev. D, 52, 3163
Cattaert T., Kourakis I., Shukla P. K., 2005, Phys. Plasmas, 12, 012319
Chian A., Kennel C. F., 1987, NASA STI/Recon. Technical Report N, 88, 16622
Galtsov D. V., Nikitina N. S., 1983, Zh. Eksperimental Teoreticheskoi Fiziki, 84, 1217
Gill R., Heyl J. S., 2009, Phys. Rev. E, 80, 036407
Heisenberg W., Euler H., 1936, Z. Phys., 98, 714
Heyl J. S., Hernquist L., 1997a, Phys. Rev. D, 55, 2449
Heyl J. S., Hernquist L., 1997b, J. Phys. A: Math. Gen., 30, 6485
Heyl J., Hernquist L., 1998, Phys. Rev. D, 58, 43005
Heyl J. S., Hernquist L., 1999, Phys. Rev. D, 59, 045005
Heyl J. S., Shaviv N. J., 2000, MNRAS, 311, 555
Heyl J. S., Shaviv N. J., 2002, Phys. Rev. D, 66, 023002
Heyl J. S., Shaviv N. J., Lloyd D., 2003, MNRAS, 342, 134
Jackson J. D., 1975, Classical Electrodynamics. Wiley, New York
Jenet F. A., Anderson S. B., Prince T. A., 2001, ApJ, 558, 302
Kozlov V. A., Litvak A. G., Suvorov E. V., 1979, Soviet J. Exp. Theor. Phys., 49, 75

Lai D., Ho W. C., 2003, Phys. Rev. Lett., 91, 071101
Lutzky M., Toll J. S., 1959, Phys. Rev., 113, 1649
Mereghetti S., 2008, A&AR, 15, 225
Mészáros P., 1992, High-Energy Radiation from Magnetized Neutron Stars. University of Chicago Press, Chicago
Meszaros P., Bonazzola S., 1981, ApJ, 251, 695
Mészáros P., Ventura J., 1978, Phys. Rev. Lett., 41, 1544
Mészáros P., Ventura J., 1979, Phys. Rev. D, 19, 3565
Meszaros P., Nagel W., Ventura J., 1980, ApJ, 238, 1066
Rajaraman R., 1982, Solitons and Instantons. North-Holland, Amsterdam
Schwinger J., 1951, Phys. Rev., 82, 664
Thompson C., Blaes O., 1998, Phys. Rev. D, 57, 3219
Thompson C., Duncan R. C., 1995, MNRAS, 275, 255
Weisskopf V., 1936, Math.-Fysiske Medd., 14, 1
Zheleznyakov V., Fabrikant A., 1982, Zh. Eksperimental Teoreticheskoi Fiziki, 82, 1366

This paper has been typeset from a TEX/LATEX file prepared by the author.